Designing 2D Vector Fields of Arbitrary Topology

H. Theisel[†]

University of Rostock, Computer Science Department, P.O. Box 999, 18051 Rostock, Germany
theisel@informatik.uni-rostock.de

Abstract

We introduce a scheme of control polygons to design topological skeletons for vector fields of arbitrary topology. Based on this we construct piecewise linear vector fields of exactly the topology specified by the control polygons. This way a controlled construction of vector fields of any topology is possible. Finally we apply this method for topology-preserving compression of vector fields consisting of a simple topology.

Keywords: *vector field, topology, critical points, separatrices, vector field compression.*

1. Introduction

The topology has been proven to be one of the most significant features of a vector field. It describes the global behavior of the vector field in terms of only a limited number of items. Hence the treatment of the topology is a popular approach in vector field visualization.

[8] introduced topological methods to vector field visualization by extracting and visualizing the topological skeleton of vector fields. Unfortunately this approach can only treat vector fields with a simple topology (i.e. consisting only of first order critical points).

In the last few years research has been done on the treatment of vector fields containing higher order critical points. In [15], higher order critical points are represented in Clifford algebras. This way higher order critical points of any index can be exactly represented whereas the number and order of the sectors of different flow behavior around the critical point could hardly be controlled. Another approach of representing higher order critical points can be found in [19]. There the critical points are represented by a piecewise linear vector field with the critical point in a vertex of the underlying triangulation. In [16] higher order interpolation techniques for vector fields are applied. This way higher order critical points may appear but their topology can hardly be controlled.

Generally the research in visualization of higher order critical points suffers from the following problem: given a vector field with higher order critical points, reliable algorithms to extract their exact topology seem not to exist. In fact, these vector fields can be described in a piecewise polynomial form of a degree larger than 1. For them, the location of critical points can be found only numerically. Moreover, there seems to be no direct way to give a complete characterization of the critical points (see section [2]). If higher order critical points cannot be extracted correctly, it is also impossible to judge if a new visualization technique is able to represent higher order critical points in a correct way.

To deal with this problem, this paper introduces a new way of obtaining vector fields: by design. While vector fields are usually obtained by measurement, simulation, or as a closed form describing certain mathematical structures, we see the following applications of a design approach of vector fields:

- Since we are able to construct vector fields of any higher order topology, and this topology is known after the design process, the constructed vector fields may serve as test data to evaluate the topological behavior of the vector field visualization technique.
- Given a vector field of a simple topology, the redesign of a vector field of its topology can be used as a compression technique for vector fields.

The approach of designing vector fields is strongly related to the ideas of designing curves and surfaces in the context of CAGD (Computer Aided Geometric Design). There

---

[†] Currently with Instituto de Cibernética, Matemática y Física, ICIMAF. C.P. 10400. La Habana, Cuba.

the curves/surfaces are designed by creating a skeleton of control polygons (for instance Bézier- or B-spline polygons). This skeleton contains the relevant information of the curve/surface in an intuitive way. See [4] for an introduction to CAGD.

To transform the CAGD approaches to vector field design, an obvious approach is to construct the topological skeleton of a vector field by a number of control polygons.

The rest of the paper is organized as follows: section 2 surveys the concepts of topology of 2D vector fields. Section 3 describes how to design the topological skeleton of a vector field by a number of simple control polygons. Section 4 shows how a vector field of exactly the specified topology is constructed out of these control polygons. In section 5 the design approach is applied to the compression of vector fields. Section 6 concludes the paper.

2. Topology of vector fields

The topology of a vector field consists of two components: critical points and separatrices. We treat these components in the following sections 2.1 and 2.2.

2.1. Critical points

To classify a critical point $\mathbf{x}_0$ of a vector field $\mathbf{v}(x,y)$ (i.e. a point $\mathbf{x}_0$ with $\mathbf{v}(\mathbf{x}_0) = (0,0)$ and $\mathbf{v}(\mathbf{x}) \neq (0,0)$ in a certain neighborhood of $\mathbf{x}_0$), sectors of different flow behavior around it have to be considered. Three kinds of sectors can be distinguished ([5]):

- In a *parabolic sector* p either all tangent curves end or all tangent curves originate in the critical point. Figure 1a shows an example.
- In a *hyperbolic sector* h all tangent curves go by the critical point, except for two tangent curves making the boundaries of the sector. One of these two tangent curves ends in the critical point while the other one originates in it. Figure 1b shows an example.
- In an *elliptic sector* e all tangent curves originate and end in it. Figure 1c shows an example.
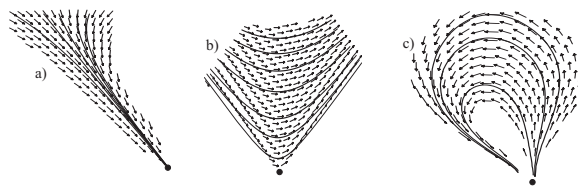

Figure 1: *Sectors of a critical point; a) parabolic sector; b) hyperbolic sector; c) elliptic sector (from [21]).*

A critical point in a 2D vector field is completely classified by specifying number and order of all sectors around it. Consider figure 2a for an example. This critical point consists

of 7 sectors in the following order: (h,e,h,e,p,h,h). (The visualization technique used for figure 2a (and the following) illustrations is called *Integrate&Draw* and is described in [13]. Here it is sufficient to mention that the behavior of the tangent curves (stream lines) can be detected quite well in this visualization.)
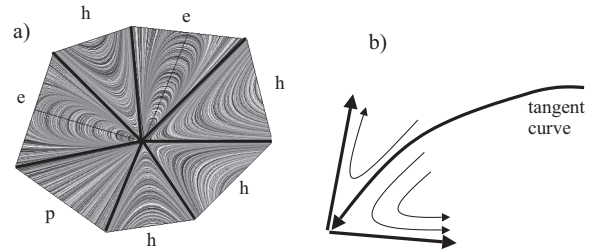

Figure 2: *a) general critical point; b) tangent curve separating two hyperbolic sectors.*

The different sectors are delimited by tangent curves originating or ending in the critical point. Figure 2b shows such a tangent curve delimiting two hyperbolic sectors.

Each critical point can be assigned with an *index* as

$$\text{index} = 1 + \frac{n_e - n_h}{2} \qquad (1)$$

where n_e is the number of elliptic sectors and n_h is the number of hyperbolic sectors. The index can also be interpreted as the number of counterclockwise revolutions made by the vectors of $\mathbf{v}$ while traveling counterclockwise on a closed curve around the critical point (the closed curve must be so tight to the critical point that no other critical points are inside it).

The index can be considered as an overview of the complexity of a critical point but does not cover the complete classification: there are critical points with different sectors but the same index. A further introduction to the classification of 2D critical points and their indices can be found in [5].

A critical point $\mathbf{x}_0 = (x_0, y_0)$ in the vector field $\mathbf{v}$ is called *first order critical point* if the Jacobian $\det(\mathbf{J_v}(\mathbf{x}_0)) = \det(\mathbf{v}_x(\mathbf{x}_0), \mathbf{v}_y(\mathbf{x}_0))$ in $\mathbf{x}_0$ does not vanish. Otherwise $\mathbf{x}_0$ is called higher order critical point. It turns out that for $\det(\mathbf{J_v}(\mathbf{x}_0)) < 0$, the critical point $\mathbf{x}_0$ consists of 4 hyperbolic sectors and has therefore an index of -1. A critical point of this classification is called a *saddle point*. In this case the eigenvectors of $\mathbf{J_v}(\mathbf{x}_0)$ denote the delimiters of the hyperbolic areas around $\mathbf{x}_0$. For $\det(\mathbf{J_v}(\mathbf{x}_0)) > 0$, the critical point $\mathbf{x}_0$ consists of one parabolic sector and has therefore an index of +1.

This classification of a first order critical point can be refined by considering the real and imaginary parts of the

eigenvalues of $\mathbf{J_v}(\mathbf{x}_0)$ which ends up in the classification introduced in [8]. Doing so, a first order critical point of an index +1 is either an attracting/repelling node, attracting/repelling focus, attracting/repelling star, or a center.

2.2. Separatrices

Separatrices are tangent curves (i.e. curves with the property that tangent direction and direction of the vector field coincide for any location of the curve) that divide the vector field into areas of different flow behavior. The literature ([9], [20], [22], [14]) describes different kinds of separatrices:

1. Each tangent curve originating/ending in the critical point and separating two sectors is a separatrix. Figure 2b illustrates a separatrix which separates two hyperbolic sectors of a critical point.

2. Separatrices do not necessarily touch any critical point. They may go "from infinity to infinity" (or from one border line of the vector field to another one). Figure 3a shows a vector field which consists of two attracting foci (see classification in [8]). The separatrix between the two critical points does not touch any of them.

3. Separatrices may originate/end in a critical point without separating sectors there. Figure 3b gives an example of that. Here we have one repelling node (middle) and two attracting nodes (left, right). Since each node consists of only one parabolic sector, the separatrices shown in the figure do not separate different sectors there.

4. Separatrices may be closed curves which do not touch any critical point. Figure 3c gives an example. Here we have two critical points: a saddle point and an attracting focus. The outer separatrix originates and ends in the saddle point and is therefore a separatrix of type 1. The inner separatrix of type 4 separates a region of inflow into the attracting focus and a region of circulation around the attracting focus.
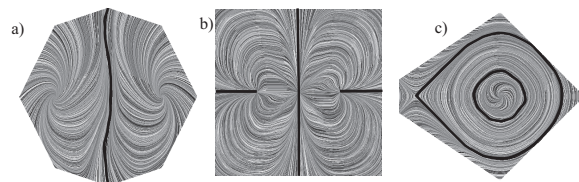
Figure 3: *Types of separatrices; a) separatrix not touching a critical point (type 2); b) separatrix not separating different sectors in the critical points (type 3); c) inner separatrix is closed curve (type 4).*

2.3. Special vector fields

Although this section 2 introduced the general concept of 2D vector field topology, many applications focus on special cases of vector fields:

- *Simple topologies*. In the following we call a vector field topology which consists only of first order critical points and separatrices of the type 1 a simple topology. Simple topologies can automatically be extracted using the approaches in [8].
- *Gradient fields* are vector fields which can be interpreted as the gradient field of a 2D scalar field. If a gradient field has a simple topology, it consists only of attracting nodes, repelling nodes and saddle points ([8]). The visualization of 3D gradient fields is treated in [1].
- *Incompressible flows* are described by a vector field $\mathbf{v}$ with $\nabla \mathbf{v} = 0$. If such a vector field has a simple topology, it consists only of saddles and centers ([8]).

3. Control polygons to describe the topological skeleton

In CAGD, the skeleton of a curve/surface is described by a set of control polygons. In a similar way we want to describe the topological skeleton of a 2D vector field as a certain set of control polygons. Since the topology of a 2D vector field consists of critical points and separatrices, we have to find control polygons both for critical points and separatrices.

3.1. Control polygons for critical points

To describe a critical point consisting of n different sectors, we use a convex closed polygon $(\mathbf{p}_0, ..., \mathbf{p}_{n-1})$ and a point $\mathbf{p}$ inside this polygon. Then $\mathbf{p}$ denotes the location of the critical point while the n separatrices are denoted by the n line segments $(\mathbf{p}, \mathbf{p}_0), (\mathbf{p}, \mathbf{p}_1), ..., (\mathbf{p}, \mathbf{p}_{n-1})$. Since each separatrix has either an inflow or outflow behavior, each of the line segments $(\mathbf{p}, \mathbf{p}_0), (\mathbf{p}, \mathbf{p}_1), ..., (\mathbf{p}, \mathbf{p}_{n-1})$ has to be marked either as inflow or outflow. Then the n areas of different flow behavior are defined by the n triangles $(\mathbf{p}, \mathbf{p}_i, \mathbf{p}_{(i+1) \bmod n})$ for $i = 0, ..., n-1$. If for an area $(\mathbf{p}, \mathbf{p}_i, \mathbf{p}_{(i+1) \bmod n})$ both separatrices $(\mathbf{p}, \mathbf{p}_i)$ and $(\mathbf{p}, \mathbf{p}_{(i+1) \bmod n})$ denote inflow (or both areas denote outflow), the triangle $(\mathbf{p}, \mathbf{p}_i, \mathbf{p}_{(i+1) \bmod n})$ describes a parabolic sector. Otherwise it has to be additionally specified whether the area should describe a hyperbolic or elliptic sector. Figure 4a illustrates the control polygon for a critical point consisting of 7 areas of different flow behavior.
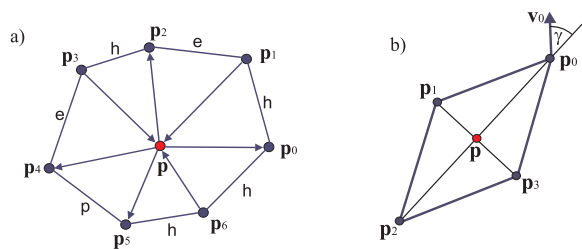
Figure 4: *a) control polygon of a critical point consisting of 7 areas of different flow behavior: (h,e,h,e,p,h,h); b) control polygon of a first order critical point of index +1.*

Special treatment is necessary for first order critical points of an index of +1. These critical points consist of only one parabolic sector; thus the general treatment described above fails. To describe them we use a rectangle $(\mathbf{p}_0, \mathbf{p}_1, \mathbf{p}_2, \mathbf{p}_3)$ with $\|\mathbf{p}_1 - \mathbf{p}_0\| = \|\mathbf{p}_2 - \mathbf{p}_1\| = \|\mathbf{p}_3 - \mathbf{p}_2\| = \|\mathbf{p}_0 - \mathbf{p}_3\|$. Then the location $\mathbf{p}$ of the critical point is the center of the rectangle. In addition, for one of the vertices (for instance $\mathbf{p}_0$) the flow direction vector $\mathbf{v}_0$ has to be specified. Then the rectangle $(\mathbf{p}_0, \mathbf{p}_1, \mathbf{p}_2, \mathbf{p}_3)$ shall describe a first order critical point in $\mathbf{p}$ in terms of the following items:

- the angle γ between $\mathbf{p}_0 - \mathbf{p}$ and $\mathbf{v}_0$
- the ratio $\|\mathbf{p}_2 - \mathbf{p}_0\| / \|\mathbf{p}_3 - \mathbf{p}_1\|$
- the orientation of the rectangle.

Figure 4b illustrates the control polygon of a first order critical point with index +1.

3.2. Control polygons for separatrices

We search for a curve scheme which has to fulfill two conditions. On one hand we need a curve scheme of a high flexibility and smoothness which can model even complicated shapes by smooth curves. On the other hand we have to keep the curve scheme as simple as necessary to construct vector fields with exactly these curves as tangent curves.

We have chosen a piecewise G^1 (tangent direction) continuous quadratic Bézier spline curve approach. As we will see later in section 4, this class of curves can nicely be incorporated into a piecewise linear vector field. The Bézier polygons of the curves are the control polygons of the separatrices. Figure 5 illustrates an example. Note that these control polygons must not intersect any of the control polygons of the critical points.
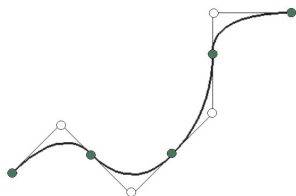
Figure 5: *Separatrix as a piecewise G^1 continuous Bézier spline curve.*

3.3. Example

To illustrate the complete construction of the topological control polygon, we construct the topological skeleton of a certain vector field of higher order topology as shown in figure 6. First we construct the control polygons of 3 higher order critical points as shown in figure 6a. As we can see in this figure, the upper critical point consists of 4 hyperbolic
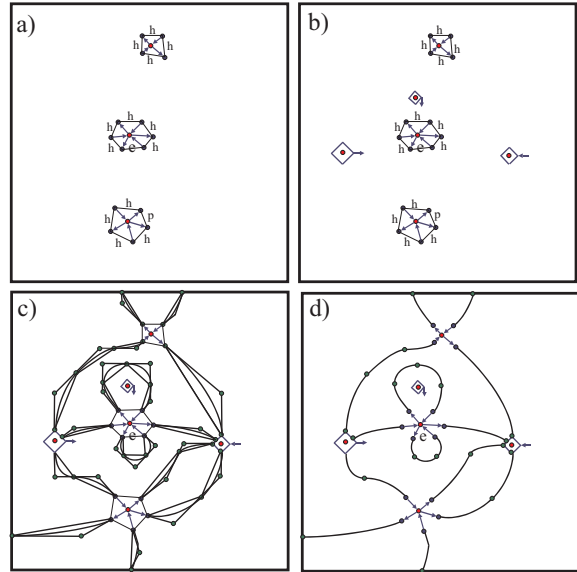
Figure 6: *Constructing a topological skeleton: a) design control polygons of general critical points; b) design control polygons of first order critical points of index +1; c) design control polygons of separatrices; d) the final topological skeleton.*

sectors, the critical point in the middle consists of 5 hyperbolic and one elliptic sectors, while the lower critical point consists of 4 hyperbolic and one parabolic sectors. In the next step, three more first order critical points of index +1 are constructed as shown in figure 6b. Then the separatrices are designed as piecewise G^1 quadratic Bézier spline curves, as shown in figure 6c. The result is a complete topological skeleton as shown in figure 6d.

This example also gives an answer to the question of what size the control polygons for the critical points should have: they should be as large as possible, but sufficiently small not to intersect each other and to leave enough space to construct the separatrices in an appropriate resolution.

4. Constructing a vector field from the topological skeleton

In this section we describe how to convert the control polygons describing the topological skeleton into a vector field of exactly the specified topology.

The vector field we obtain will be a *piecewise linear vector field*. To apply this class of vector fields, two problems have to be solved:

- How to describe higher order critical points using piecewise linear vector fields?
- How to describe piecewise quadratic separatrices using piecewise linear vector fields?

These two problems are treated in the sections 4.1 and 4.2. Then section 4.3 describes the algorithm to construct a piecewise linear vector field of a given topological skeleton.

4.1. Higher order critical points in piecewise linear vector fields

To describe higher order critical points by piecewise linear vector fields we adapt the main idea of [19]. Given the closed polygon $(\mathbf{p}_0, ..., \mathbf{p}_{n-1})$ and the critical point $\mathbf{p}$ inside this polygon, we construct the following initial triangulation: $\mathbf{p}$ is assigned with the zero vector $\mathbf{v} = (0,0)^T$; $\mathbf{p}_i$ is assigned with the vector $\mathbf{v}_i = \lambda_i (\mathbf{p}_i - \mathbf{p})$ with $\lambda_i \neq 0$ for $i = 0, ..., n-1$. The sign of λ_i depends on the inflow/outflow behavior of the separatrix $(\mathbf{p}, \mathbf{p}_i)$. A positive λ_i gives an outflow separatrix while a negative λ_i gives an inflow separatrix. The magnitudes of λ_i can be freely chosen at this state of the construction process. To avoid numerical problems, it is recommended that all λ_i have approximately the same magnitude. For the following applications we have chosen $\lambda_i = \pm 1$. Then the initial triangulation to describe the critical point is given by the triangles $(\mathbf{p}, \mathbf{p}_i, \mathbf{p}_{(i+1) \bmod n})$ with the assigned vectors $(\mathbf{v}, \mathbf{v}_i, \mathbf{v}_{(i+1) \bmod n})$ for $i = 0, ..., n-1$. Figure 7a illustrates this initial triangulation for the example shown in figure 4a.
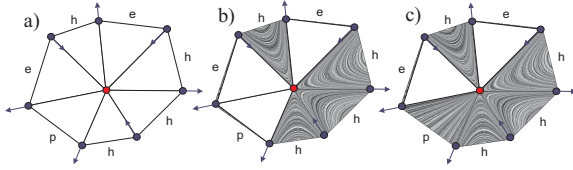
Figure 7: *a) initial triangulation for the example shown in figure 4a; b) linear interpolation in all hyperbolic sectors; c) linear interpolation in all parabolic sectors.*

If a sector $(\mathbf{p}, \mathbf{p}_i, \mathbf{p}_{(i+1) \bmod n})$ describes a hyperbolic sector, a linear interpolation of the vectors $(\mathbf{v}, \mathbf{v}_i, \mathbf{v}_{(i+1) \bmod n})$ inside the triangle $(\mathbf{p}, \mathbf{p}_i, \mathbf{p}_{(i+1) \bmod n})$ is applied. Figure 7b illustrates this for all hyperbolic sectors of the example. Also a linear interpolation is applied for all parabolic sectors, as shown in figure 7c.

If the sector $(\mathbf{p}, \mathbf{p}_i, \mathbf{p}_{(i+1) \bmod n})$ describes an elliptic area, the triangle $(\mathbf{p}, \mathbf{p}_i, \mathbf{p}_{(i+1) \bmod n})$ has to be refined by inserting an auxiliary point $\mathbf{q}_i$ with an assigned auxiliary vector $\mathbf{w}_i$, and considering the two new triangles $(\mathbf{p}, \mathbf{p}_i, \mathbf{q}_i)$ and $(\mathbf{p}, \mathbf{q}_i, \mathbf{p}_{(i+1) \bmod n})$. Describing $\mathbf{q}_i$ and $\mathbf{w}_i$ by

$$\mathbf{q}_i = \alpha \mathbf{p} + \beta \mathbf{p}_i + \gamma \mathbf{p}_{(i+1) \bmod n}$$
$$\mathbf{w}_i = -\left(\delta \mathbf{v}_i + \varepsilon \mathbf{v}_{(i+1) \bmod n}\right)$$

with $\alpha + \beta + \gamma = 1$ and $\beta, \gamma, \delta, \varepsilon > 0$, we formulate the following constraints for $\mathbf{q}_i, \mathbf{w}_i$:

- The triangles $(\mathbf{p}, \mathbf{p}_i, \mathbf{q}_i)$ and $(\mathbf{p}, \mathbf{q}_i, \mathbf{p}_{(i+1) \bmod n})$ must not create new separatrices by applying a linear interpolation inside them, i.e.

$$\det((1-t)\mathbf{p}_i + t\mathbf{q}_i - \mathbf{p}, (1-t)\mathbf{v}_i + t\mathbf{w}_i) \neq 0$$
$$\det((1-t)\mathbf{q}_i + t\mathbf{p}_{(i+1) \bmod n} - \mathbf{p},$$
$$(1-t)\mathbf{w}_i + t\mathbf{v}_{(i+1) \bmod n}) \neq 0$$

for $0 < t < 1$.
- The tangent curves of the piecewise linear vector field over the two triangles $(\mathbf{p}, \mathbf{p}_i, \mathbf{q}_i)$ and $(\mathbf{p}, \mathbf{q}_i, \mathbf{p}_{(i+1) \bmod n})$ which pass over the line $(\mathbf{p}, \mathbf{q}_i)$ are curvature continuous (see [18] for computing the curvature of tangent curves)
- $\delta^2 + \varepsilon^2 \to \min$.

These three conditions form a minimization problem with boundary conditions. It has a unique solution for $\alpha, \beta, \gamma, \delta, \varepsilon$ and therefore for $\mathbf{q}_i$ and $\mathbf{w}_i$:

$$\mathbf{q}_i = \frac{1}{2}\left(\mathbf{p}_i + \mathbf{p}_{(i+1) \bmod n}\right)$$

$$\mathbf{w}_i = \begin{cases} \frac{1}{2}\frac{\lambda_i}{\lambda_{(i+1) \bmod n}}\left(\mathbf{v}_i + \mathbf{v}_{(i+1) \bmod n}\right) \\ \qquad\qquad \text{for} \quad -\frac{\lambda_i}{\lambda_{(i+1) \bmod n}} \geq 1 \\[2ex] \frac{1}{2}\frac{\lambda_{(i+1) \bmod n}}{\lambda_i}\left(\mathbf{v}_i + \mathbf{v}_{(i+1) \bmod n}\right) \\ \qquad\qquad \text{for} \quad -\frac{\lambda_i}{\lambda_{(i+1) \bmod n}} < 1 \end{cases}$$

where $\lambda_i, \lambda_{(i+1) \bmod n}$ are obtained from $\mathbf{v}_i = \lambda_i(\mathbf{p}_i - \mathbf{p})$ and $\mathbf{v}_{(i+1) \bmod n} = \lambda_{(i+1) \bmod n}(\mathbf{p}_{(i+1) \bmod n} - \mathbf{p})$. Figure 8 illustrates this.
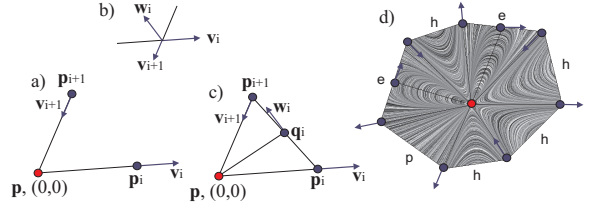
Figure 8: *Constructing an elliptic area: a) initial sector; b) location of $\mathbf{w}_i$ relative to $\mathbf{v}_i$ and $\mathbf{v}_{i+1}$; c) refined triangulation after inserting $\mathbf{q}_i$ with $\mathbf{w}_i$; d) application to the example in figure 4a.*

If the critical point to be described is a first order critical point of index +1, we construct a piecewise linear vector field out of its topological skeleton shown in figure 4b in the following way: the vectors $\mathbf{v}_i$ assigned to the control points $\mathbf{p}_i$ $(i = 1, 2, 3)$ are computed by

$$\|\mathbf{v}_i\| = \|\mathbf{v}_0\|$$
$$\text{angle}(\mathbf{v}_i, \mathbf{p}_i - \mathbf{p}) = \text{angle}(\mathbf{v}_0, \mathbf{p}_0 - \mathbf{p})$$

Then a piecewise linear interpolation over the two subtriangles $(\mathbf{p}_0, \mathbf{p}_1, \mathbf{p}_3)$ and $(\mathbf{p}_1, \mathbf{p}_2, \mathbf{p}_3)$ gives the desired first

order critical point. Figure 9 illustrates this. This way it can be shown that any first order critical point can be uniquely described by a configuration of the control polygon $(\mathbf{p}_0, \mathbf{p}_1, \mathbf{p}_2, \mathbf{p}_3)$.
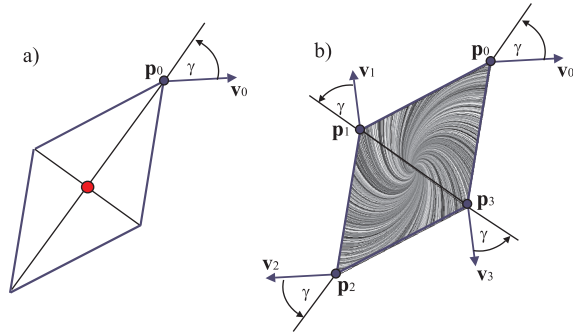
Figure 9: *Constructing a first order critical point of index +1; a) control polygon; b) resulting piecewise linear vector field.*

4.2. Piecewise quadratic separatrices in piecewise linear vector fields

In [12] it has been shown that the tangent curve of a linear vector field is in general a certain exponential curve. In order to describe a separatrix (i.e. a special tangent curve) as a parabola segment, we search for a useful special configuration of the vector field where a tangent curve simplifies to a parabola. We formulate

Theorem 1 Let a non-degenerate 2D triangle $(\mathbf{p}_0, \mathbf{p}_1, \mathbf{p}_2)$ assigned with the 2D vectors $(\mathbf{v}_0, \mathbf{v}_1, \mathbf{v}_2)$ have the following properties:

$$\mathbf{v}_0 = \lambda_0 (\mathbf{p}_1 - \mathbf{p}_0) \tag{2}$$

$$\mathbf{v}_2 = \lambda_2 (\mathbf{p}_2 - \mathbf{p}_1) \tag{3}$$

$$\mathbf{v}_1 = \frac{1}{2} (\lambda_2 (\mathbf{p}_1 - \mathbf{p}_0) + \lambda_0 (\mathbf{p}_2 - \mathbf{p}_1)) \tag{4}$$

for certain $\lambda_0, \lambda_2 > 0$. Applying a linear interpolation of the vectors $(\mathbf{v}_0, \mathbf{v}_1, \mathbf{v}_2)$ inside the triangle $(\mathbf{p}_0, \mathbf{p}_1, \mathbf{p}_2)$, the following statements for the resulting linear vector field hold:

1. The tangent curve passing through $\mathbf{p}_0$ passes through $\mathbf{p}_2$ as well.
2. The tangent curve through $\mathbf{p}_0$ and $\mathbf{p}_2$ has the same shape (but not necessarily the same parameterization) as the parabola defined by the Bézier points $(\mathbf{p}_0, \mathbf{p}_1, \mathbf{p}_2)$.

To prove theorem 1 we have to show that for every point on the parabola defined by the Bézier points $(\mathbf{p}_0, \mathbf{p}_1, \mathbf{p}_2)$ the tangent direction and the direction of $\mathbf{v}$ at the curve location coincide. Let

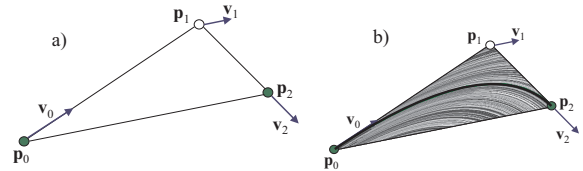$$\mathbf{x}(t) = \sum_{i=0}^{2} B_i^2(t)\, \mathbf{p}_i$$

be the parabola where $B_i^2(t)$ are the Bernstein polynomials (see [4]). Since $\sum_{i=0}^{2} B_i^2(t) \equiv 1$, the Bernstein polynomials can be considered as the barycentric coordinates relative to the points $\mathbf{p}_i$. Thus we obtain

$$\mathbf{v}(\mathbf{x}(t)) = \sum_{i=0}^{2} B_i^2(t)\, \mathbf{v}_i. \tag{5}$$

Inserting (2) - (4) into (5) gives

$$\begin{aligned} \mathbf{v}(\mathbf{x}(t)) &= \left((1-t)\lambda_0 + t\lambda_2 \right) \\ &\quad \cdot \left((1-t)(\mathbf{p}_1 - \mathbf{p}_0) + t(\mathbf{p}_2 - \mathbf{p}_1) \right) \\ &= \frac{1}{2} \left((1-t)\lambda_0 + t\lambda_2 \right) \dot{\mathbf{x}}(t) \end{aligned} \tag{6}$$

which proves the theorem. Figure 10 illustrates theorem 1.

Figure 10: *Illustration of theorem 1; a) illustration of conditions (2) - (4); b) resulting vector field and parabola shaped tangent curve.*

Theorem 1 can easily be used to construct a piecewise linear vector field which describes a G^1 piecewise quadratic separatrix of a given skeleton. Figure 11 illustrates this for the separatrix shown in figure 5.

4.3. The algorithm

Now we can formulate the *algorithm* to construct a piecewise linear vector field of a given topological skeleton:

1. Construct the piecewise linear vector field inside the control polygons of all general critical points.
2. Construct the piecewise linear vector field inside the control polygons of all first order critical points of index +1.
3. Construct the piecewise linear vector field describing all separatrices.
4. Specify the flow direction vector in additional interesting points and in the corner vertices of the domain.
5. Triangulate the remaining parts of the vector field using only the already defined vertices, and apply a piecewise linear interpolation on this triangulation. To do this, we used a Delaunay triangulation. In this step no further critical points must be obtained. For a correct and complete
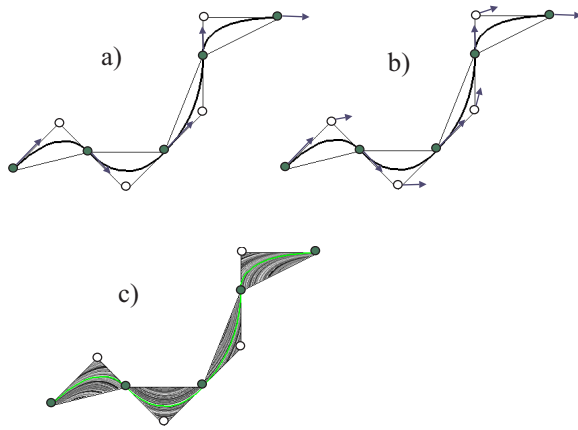
Figure 11: *Constructing a piecewise linear vector field consisting of a piecewise G^1 quadratic separatrix; a) construct vectors at the junction points using (2) and (3); b) construct vectors at intermediate points using (4); c) resulting piecewise linear vector field and separatrix.*

Figure 12: *Constructing the piecewise linear vector field for the topological skeleton of figure 6; a) construct piecewise linear vector field for general critical points; b) construct piecewise linear vector field for first order critical points of index +1; c) construct piecewise linear vector field for separatrices; d) piecewise linear interpolation after Delaunay triangulating the remaining parts; e) final vector field consists of 79 vertices and 138 triangles; f) curvature plot of e).*
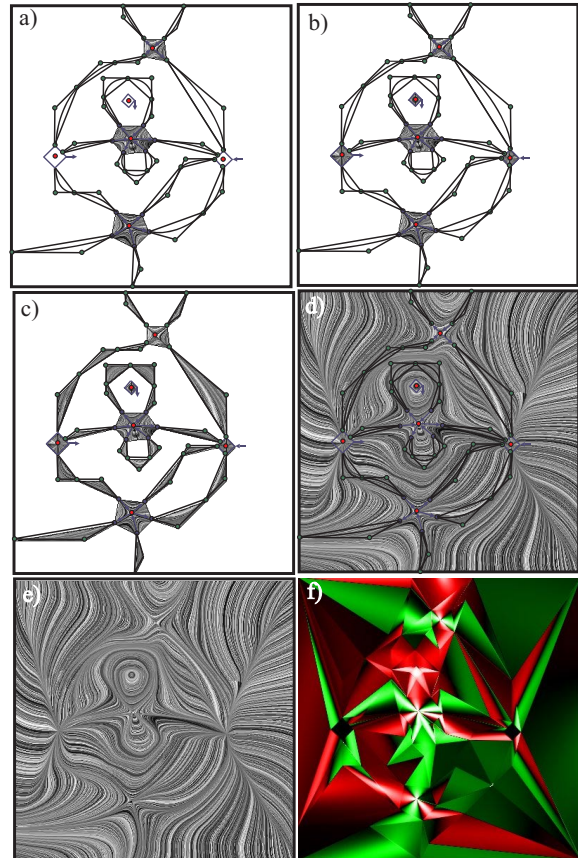
topological skeleton the appearance of new critical points can be prevented by interactively introducing new auxiliary vertices and their assigned vectors in the still uncovered areas of the vector field.

The result of this algorithm is a piecewise linear vector field of exactly the same topology as specified in the topological skeleton. Figure 12 illustrates this algorithm by constructing a piecewise linear vector field to the topological skeleton introduced in figure 6. This vector field with 3 general critical points and 3 first order critical points is constructed as piecewise linear vector field consisting of 79 vertices and 138 triangles.

5. Simplification and compression of vector fields

In recent years the simplification and compression of vector fields became a popular research topic in scientific visualization. Flow data sets (and the vector fields derived from them) are continuously growing, such that their simplification and compression becomes significant in the visualization process.

Simplification of a vector field means finding a new vector field which keeps the most important properties but skips the less important details. In [2] the topology of a 2D vector field is simplified using area metrics. There the input vector field has to be a gradient field of a simple topology (i.e. only first order critical points and separatrices of type 1). The output vector field is a simple vector field with a reduced number of critical points. In [3] the topology of simple gradient fields

is simplified by using Morse complexes. In [19] a vector field of a rich simple topology (i.e. a high number of first order critical points) is simplified by replacing clusters of first order critical points by a higher order critical point. Note that a topological simplification of a vector field does not necessarily cause a compression. For instance the simplified vector fields in [19] may even be bigger than the originals.

To compress a vector field means to find a new vector field of smaller size which keeps important properties of the original one. Compression algorithms are well-researched in the context of images and scalar fields. So the first approaches on compressing vector fields focused on adapting compression techniques of other data classes. This way [7], [17] and [6]

construct hierarchies of compressed vector fields. Unfortunately, these techniques do not consider the topology of vector fields. In fact, the compressed vector fields may have significant different topologies than the originals.

[11] introduces the first approach to compress a vector field while preserving its topology by applying a bottom-up clustering similar to [17]. Based on a topology based metric for vector fields introduced in [10], compressed vector fields with the same critical points classification are obtained. The behavior of separatrices is not considered in [11]. For vector fields with a poor topology (i.e. only a few critical points and separatrices), significant compression rates can be achieved.

In the remaining part of this section we want to apply the results of sections 3 and 4 to introduce a new topology-preserving compressing technique for 2D vector fields of a simple topology. Given a 2D vector field of a simple topology, its topological skeleton can be extracted automatically (see [8]). The result of this extraction process is the exact classification of all first order critical points, and numerically integrated separatrices. To convert this into a set of control polygons described in section 3, the numerically integrated separatrices have to be replaced by piecewise G^1 quadratic curve segments. This may be done interactively or automatically by placing an appropriate number of sample points on the numerically integrated curve and declaring them as junction points of the parabola segments.

After the topological skeleton is constructed as shown in section 3, a vector field of exactly this topology can be constructed following the approach of section 4. The new vector field obtained this way has exactly the same topology as the original one. It turns out that for vector fields with rather poor topology, the new vector field is a compressed version the of original one.

To demonstrate this compression algorithm we consider the gradient field from one of Franke's data sets

$$s(x,y) = \quad \frac{3}{4} e^{-\frac{(9x-2)^2+(9y-2)^2}{4}} + \frac{1}{2} e^{-\frac{(9x-7)^2+(9y-3)^2}{4}} \quad (7)$$
$$-\frac{1}{5} e^{-(9x-4)^2+(9y-7)^2} + \frac{3}{4} e^{-\frac{(9x+1)^2}{49}-\frac{(9y+1)^2}{10}}$$

in the domain $[0,1]^2$, sampled by a 38 x 38 grid. This vector field was already addressed in [11] where a topology-preserving compression ratio of 90% was achieved. The vector field (7) is shown in figure 13a. Figure 13b shows its curvature plot. (The curvature of a vector field is studied in [18]. Here it is sufficient to mention that the curvature of the tangent curves are computed and color coded in every point of the vector field in the following way: positive curvature gets red color, negative color gets green color, the higher the curvature the brighter the color is. This way critical points appear as highlights, and the underling grid becomes visible due to the fact that tangent curves are generally not curvature continuous in piecewise (bi)linear vector fields.)
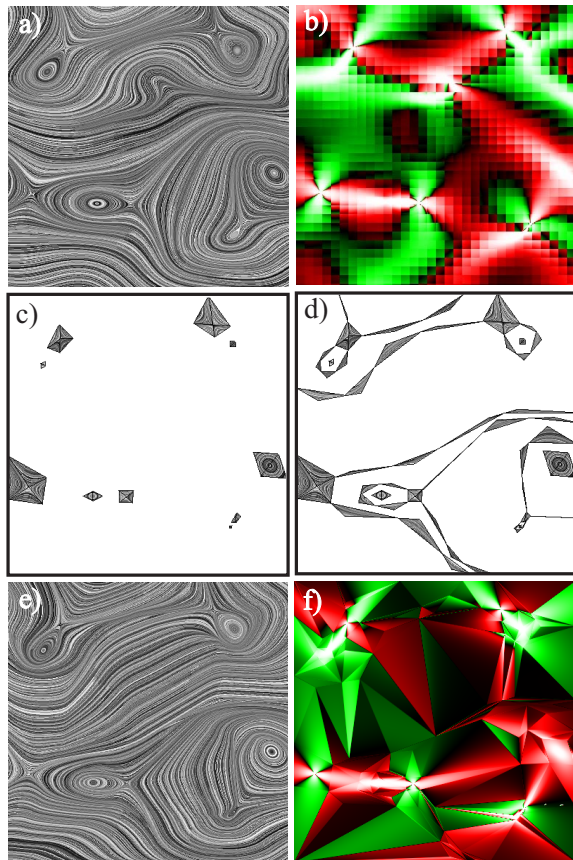
After automatically extracting the topology, the first order critical points are modelled as shown in figure 13c. Figure 13d shows how the separatrices are modelled in the piecewise linear vector field. (Since some of the separatrices in this vector field are approximately straight lines, the triangles to represent them collapse to line segments.) Figure 13e shows the final piecewise linear vector field which consists of 40 vertices and 68 triangles. Thus the compression ratio to the original vector field is 95%. Some visual differences between figure 13e and the original in figure 13a appear in regions rather far away from any critical point or separatrix. This is due to the fact that in these regions no information at all is incorporated into the compression process. However, the topology (and thus the general flow behavior) of the original and the compressed vector field are guaranteed to be the same. Figure 13f shows the curvature plot of figure 13e.
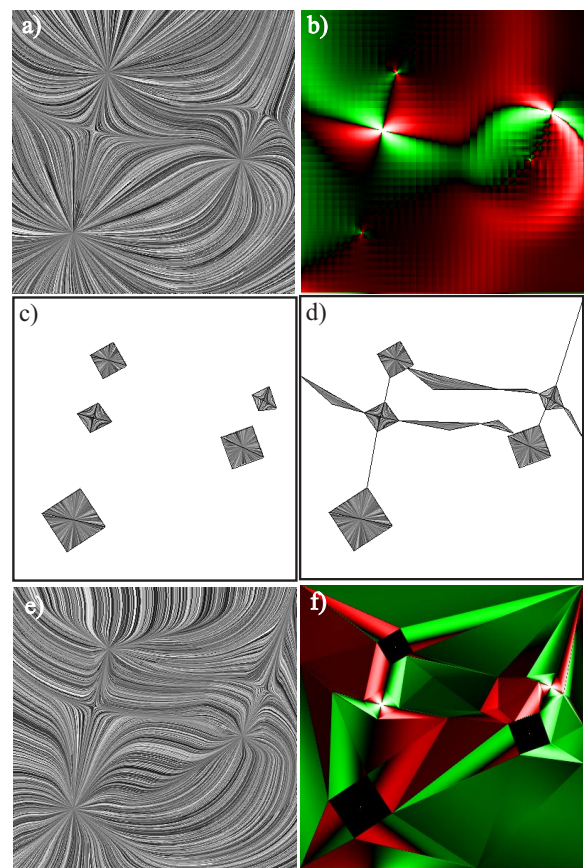
Figure 13: *a) vector field (7) on a 38 x 38 regular grid: 1444 grid points; b) curvature plot of a); c) remodelling the critical points as piecewise linear vector field; d) remodelling the separatrices as piecewise linear vector field; e) complete remodelled piecewise linear vector field consists of 40 vertices and 68 triangles: compression ratio 95%; f) curvature plot of e).*

Another example of a vector field with a richer topology is shown in figure 14. Figure 14a shows a fragment of a data set which describes the flow of a bay area of the Baltic Sea near Greifswald (Germany). It consists of a regular 34 x 34 grid and has therefore 1056 grid points. Figure 14b shows its curvature plot. Figure 14c shows the construction of the critical points as a piecewise linear vector field. Figure 14d shows the construction of the separatrices. Figure 14e shows the complete remodeled piecewise linear vector field consisting of 124 vertices and 226 triangles. This gives a compression ratio of 79% in comparison to figure 14a. The curvature plot in figure 14f both reveals the underlying triangulation and shows the effect of compression in comparison to figure 14b.

The topology-preserving compression algorithm introduced here gives high compression rates if the original vector field has a rather poor topology. This means only few information is necessary to describe the topology. In fact, the compression ratios are higher than the only comparable approach in [11] although our approach also considers the separatrices which are omitted in [11].

However, for a rich topology a higher amount of information is necessary to describe it. Hence the compression ratios are lower. In fact, for very rich topologies even negative compression ratios are possible. (Imagine for instance a piecewise bilinear vector field with two critical points in each cell of the underlying grid.) However, topology extraction algorithms have been developed especially for vector fields with rather simple topologies. Nevertheless, the avoidance of negative compression ratios of our algorithm should be part of future research.

6. Conclusions and future research

We have presented an approach to design 2D vector fields of any topology out of a set of control polygons describing the topological skeleton. This approach can deal with all kinds of critical points and separatrices. The result is a C^0 continuous piecewise linear vector field. Due to its well-defined topology it can serve as input data to evaluate the topological behavior of vector field visualization techniques. Furthermore we applied the design approach as a topology-preserving compression technique for vector fields with a simple topology. This way the complete topology (i.e. critical points and separatrices) is preserved during compression. For vector fields with a rather poor topology, significant compression ratios can be achieved.

For future research, the following problems have to solved concerning the compression approach:

- To reduce the visual differences between the original and the compressed vector field, additional sample points can be incorporated into the triangulation. These sample points points might be chosen automatically or interactively. This way it might even be possible to introduce hierarchies of newly inserted sample points.
- To avoid possible negative compression ratios, approaches should be developed to apply the method only in regions of locally poor topology and leave the remaining regions untouched.
- Another way to avoid negative compression ratios is to apply a controlled topology simplification algorithm before applying the compression algorithm.

7. Acknowledgements

Figure 14: *a) fragment of a flow data set of the Baltic Sea consisting of a 34 x 34 regular grid: 1056 grid points; b) curvature plot of a); c) remodelling the critical points as piecewise linear vector field; d) remodelling the separatrices as piecewise linear vector field; e) complete remodelled piecewise linear vector field consists of 124 vertices and 226 triangles: compression ratio 79%; f) curvature plot of e); data set provided by Department of Mathematics, University of Rostock*

References

1. C.L. Bajaj, V. Pascucci, and D.R. Schikore. Visualization of scalar topology for structural enhancement. In D. Ebert, H. Hagen, and H. Rushmeier, editors, *Proc. IEEE Visualization '98*, pages 51–58, Los Alamitos, 1998. IEEE Computer Society Press. 3

2. W. de Leeuw and R. van Liere. Collapsing flow topology using area metrics. In D. Ebert, M. Gross, and B. Hamann, editors, *Proc. IEEE Visualization '99*, pages 149–354, Los Alamitos, 1999. 7

3. H. Edelsbrunner, J. Harer, and A. Zomorodian. Hierarchical morse complexes for piecewise linear 2-manifolds. In *Proc. 17th Sympos. Comput. Geom. 2001*, 2001. 7

4. G. Farin. *Curves and Surfaces for Computer Aided Geometric Design*. Academic Press, Boston, 4th edition, 1997. 2, 6

5. P.A. Firby and C.F. Gardiner. *Surface Topology*, chapter 7, pages 115–135. Ellis Horwood Ltd., 1982. Vector Fields on Surfaces. 2

6. H. Garcke, T. Preusser, M. Rumpf, A. Telea, U. Weikardt, and J. van Wijk. A continuous clustering method for vector fields. In T. Ertl, B. Hamann, and A. Varshney, editors, *Proc. IEEE Visualization 2000*, pages 351–358, 2000. 7

7. B. Heckel, G.H. Weber, B. Hamann, and K.I.Joy. Construction of vector field hierarchies. In D. Ebert, M. Gross, and B. Hamann, editors, *Proc. IEEE Visualization '99*, pages 19–26, Los Alamitos, 1999. 7

8. J. Helman and L. Hesselink. Representation and display of vector field topology in fluid flow data sets. *IEEE Computer*, 22(8):27–36, August 1989. 1, 3, 8

9. D.N. Kenwright, C. Henze, and C. Levit. Feature extraction of separation and attachment lines. *IEEE Transactions on Visualization and Computer Graphics*, 5(2):135–144, 1999. 3

10. Y. Lavin, R.K. Batra, and L. Hesselink. Feature comparisons of vector fields using earth mover's distance. In D. Ebert, H. Hagen, and H. Rushmeier, editors, *Proc. IEEE Visualization '98*, pages 103–109, Los Alamitos, 1998. IEEE Computer Society Press. 8

11. S.K. Lodha, J.C. Renteria, and K.M. Roskin. Topology preserving compression of 2d vector fields. In T. Ertl, B. Hamann, and A. Varshney, editors, *Proc. IEEE Visualization 2000*, pages 343–350, 2000. 8, 9

12. G.M. Nielson. Tools for computing tangent curves and topological graphs for visualizing piecewise linearly varying vector fields over triangulated domains. In G.M. Nielson, H. Hagen, and H. Müller, editors, *Scientific Visualization*, pages 527–562. IEEE Computer Society, 1997. 6

13. C. Perez Risquet. Visualizing 2D flows: Integrate and Draw. In *Proceedings 9th Eurographics Workshop on Visualization in Scientific Computing*, pages 57–67, 1998. 2

14. G. Scheuermann, B. Hamann, K. Joy, and W. Kollman. Visualizing local vector field topology. *Journal of Electronic Imaging*, 9(4):356–367, 2000. 3

15. G. Scheuermann, H. Krüger, M. Menzel, and A. Rockwood. Visualizing non-linear vector field topology. *IEEE Transactions on Visualization and Computer Grapics*, 4(2):109–116, 1998. 1

16. G. Scheuermann, X. Tricoche, and H. Hagen. C1-interpolation for vector field topology interpolation. In D. Ebert, M. Gross, and B. Hamann, editors, *Proc. IEEE Visualization '99*, pages 271–278, Los Alamitos, 1999. 1

17. A. Telea and J.J. van Wijk. Simplified representation of vector fields. In D. Ebert, M. Gross, and B. Hamann, editors, *Proc. IEEE Visualization '99*, pages 35–42, Los Alamitos, 1999. 7, 8

18. H. Theisel. *Vector Field Curvature and Applications*. PhD thesis, University of Rostock, November 1995. 5, 8

19. X. Tricoche, G. Scheuermann, and H. Hagen. A topology simplification method for 2d vector fields. In T. Ertl, B. Hamann, and A. Varshney, editors, *Proc. IEEE Visualization 2000*, pages 359–366, 2000. 1, 5, 7

20. I. Trotts, D. Kenwright, and R. Haimes. Critical points at infinity: a missing link in vector field topology. In *Proc. NSF/DoE Lake Tahoe Workshop on Hierarchical Approximation and Geometrical Methods for Scientific Visualization*, 2000. available at http://graphics.cs.ucdavis.edu/ hvm00/program.html. 3

21. T. Weinkauf. Krümmungsvisualisierung für 3D-Vektorfelder. Diplomarbeit, University of Rostock, Computer Science Department, 2000. (in German). 2

22. T. Wischgoll and G. Scheuermann. Detection and visualization of closed streamlines in planar flows. *IEEE Transactions on Visualization and Computer Graphics*, 7(2):165–172, 2001. 3